Spherical wavelet-Bayesian cosmic string tension estimation

Jason McEwen[1]

http://www.jasonmcewen.org/

In collaboration with
Stephen Feeney[1], Hiranya Peiris[1], Yves Wiaux[2],
Christophe Ringeval[3] & François Bouchet[4]

[1] Department of Physics and Astronomy, University College London (UCL)
[2] Institute of Electrical Engineering, Ecole Polytechnique Federale de Lausanne (EPFL)
[3] Institute of Mathematics and Physics, Louvain University
[4] Institut d'Astrophysique de Paris, Université Pierre et Marie Curie

Big Bang, Big Data, Big Computers :: Paris :: September 2012

Outline

Outline

Cosmic strings

- Symmetry breaking phase transitions in the early Universe $\rightarrow$ topological defects.
- Cosmic strings well-motivated phenomenon that arise when axial or cylindrical symmetry is broken $\rightarrow$ line-like discontinuities in the fabric of the Universe.
- Although we have not yet observed cosmic strings, we have observed string-like topological defects in other media, e.g. ice and liquid crystal.
- Cosmic strings are distinct to the fundamental superstrings of string theory.
- However, recent developments in string theory suggest the existence of macroscopic superstrings that could play a similar role to cosmic strings.
- **The detection of cosmic strings would open a new window into the physics of the Universe!**

Figure: Optical microscope photograph of a thin film of freely suspended nematic liquid crystal after a temperature quench. Credit: Chuang *et al.* (1991).

Cosmic strings

- Symmetry breaking phase transitions in the early Universe $\rightarrow$ topological defects.
- Cosmic strings well-motivated phenomenon that arise when axial or cylindrical symmetry is broken $\rightarrow$ line-like discontinuities in the fabric of the Universe.
- Although we have not yet observed cosmic strings, we have observed string-like topological defects in other media, e.g. ice and liquid crystal.
- Cosmic strings are distinct to the fundamental superstrings of string theory.
- However, recent developments in string theory suggest the existence of macroscopic superstrings that could play a similar role to cosmic strings.
- The detection of cosmic strings would open a new window into the physics of the Universe!

Figure: Optical microscope photograph of a thin film of freely suspended nematic liquid crystal after a temperature quench. Credit: Chuang *et al.* (1991).

Cosmic strings

- Symmetry breaking phase transitions in the early Universe $\rightarrow$ topological defects.
- Cosmic strings well-motivated phenomenon that arise when axial or cylindrical symmetry is broken $\rightarrow$ line-like discontinuities in the fabric of the Universe.
- Although we have not yet observed cosmic strings, we have observed string-like topological defects in other media, e.g. ice and liquid crystal.
- Cosmic strings are distinct to the fundamental superstrings of string theory.
- However, recent developments in string theory suggest the existence of macroscopic superstrings that could play a similar role to cosmic strings.
- **The detection of cosmic strings would open a new window into the physics of the Universe!**

Figure: Optical microscope photograph of a thin film of freely suspended nematic liquid crystal after a temperature quench. Credit: Chuang *et al.* (1991).

Observational signatures of cosmic strings

- Spacetime about a cosmic string is canonical, with a three-dimensional wedge removed (Vilenkin 1981).
- Strings moving transverse to the line of sight induce line-like discontinuities in the CMB (Kaiser & Stebbins 1984).
- The amplitude of the induced contribution scales with $G\mu$, the string tension.

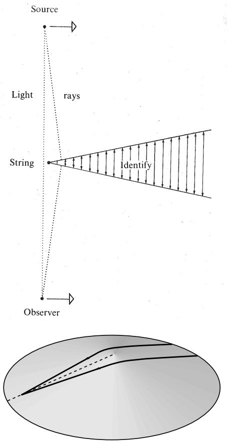

Figure: Spacetime around a cosmic string. Credit: Kaiser & Stebbins 1984, DAMTP.

Observational signatures of cosmic strings

- Make contact between theory and data using high-resolution simulations.
- High-resolution full-sky simulations created by Christophe Ringeval.

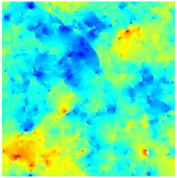

(a) Flat patch (Fraisse *et al.* 2008)

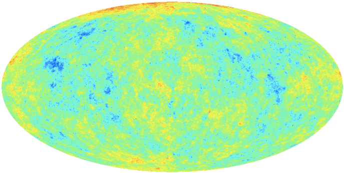

(b) Full-sky (Ringeval *et al.* 2012)

Figure: Cosmic string simulations.

Observational signatures of cosmic strings

- Make contact between theory and data using high-resolution simulations.
- High-resolution full-sky simulations created by Christophe Ringeval.

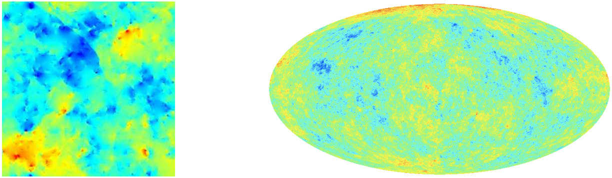

(a) Flat patch (Fraisse *et al.* 2008) (b) Full-sky (Ringeval *et al.* 2012)

Figure: Cosmic string simulations.

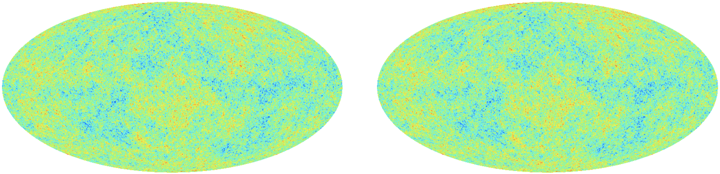

(a) CMB (b) CMB with embedded string

Figure: CMB simulation with string contribution ($G\mu = 5 \times 10^{-7}$) embedded .

Outline

Why wavelets?

Fourier (1807)

Haar (1909)

Morlet and Grossman (1981)

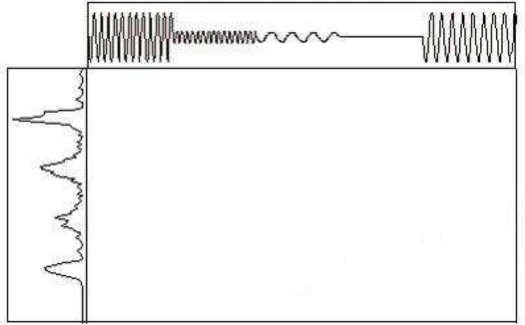

Figure: Fourier vs wavelet transform (credit: `http://www.wavelet.org/tutorial/`)

Why wavelets?

Fourier (1807)

Haar (1909)

Morlet and Grossman (1981)

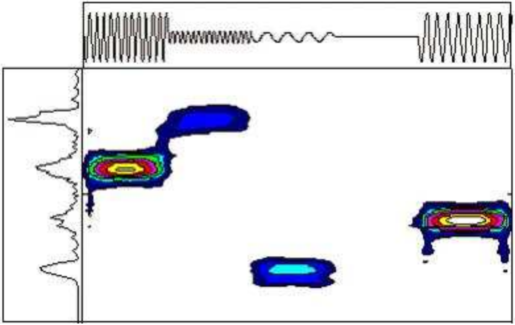

Figure: Fourier vs wavelet transform (credit: `http://www.wavelet.org/tutorial/`)

Wavelet transform in Euclidean space

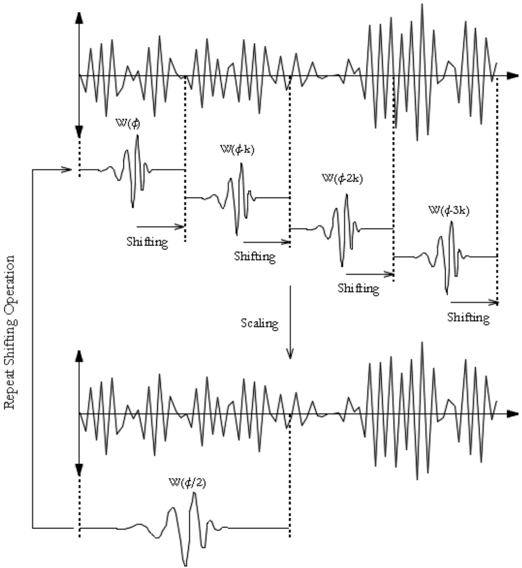

Figure: Wavelet scaling and shifting (image from http://www.wavelet.org/tutorial/)

Continuous wavelets on the sphere

- First natural wavelet construction on the sphere was derived in the seminal work of Antoine and Vandergheynst (1998) (reintroduced by Wiaux 2005).
- Construct wavelet atoms from affine transformations (dilation, translation) on the sphere of a mother wavelet.
- The natural extension of translations to the sphere are rotations. Rotation of a function f on the sphere is defined by

$$[\mathcal{R}(\rho)f](\omega) = f(\rho^{-1}\omega), \quad \omega = (\theta, \varphi) \in \mathrm{S}^2, \quad \rho = (\alpha, \beta, \gamma) \in \mathrm{SO}(3) .$$

- How define dilation on the sphere?
- The spherical dilation operator is defined through the conjugation of the Euclidean dilation and stereographic projection Π:

$$\mathcal{D}(a) \equiv \Pi^{-1}\, d(a)\, \Pi .$$

Continuous wavelets on the sphere

- First natural wavelet construction on the sphere was derived in the seminal work of Antoine and Vandergheynst (1998) (reintroduced by Wiaux 2005).
- Construct wavelet atoms from affine transformations (dilation, translation) on the sphere of a mother wavelet.
- The natural extension of translations to the sphere are rotations. Rotation of a function f on the sphere is defined by

$$[\mathcal{R}(\rho)f](\omega) = f(\rho^{-1}\omega), \quad \omega = (\theta, \varphi) \in \mathrm{S}^2, \quad \rho = (\alpha, \beta, \gamma) \in \mathrm{SO}(3) \, .$$

- How define dilation on the sphere?
- The spherical dilation operator is defined through the conjugation of the Euclidean dilation and stereographic projection Π:

$$\mathcal{D}(a) \equiv \Pi^{-1} \, d(a) \, \Pi \, .$$

Continuous wavelets on the sphere

- First natural wavelet construction on the sphere was derived in the seminal work of Antoine and Vandergheynst (1998) (reintroduced by Wiaux 2005).
- Construct wavelet atoms from affine transformations (dilation, translation) on the sphere of a mother wavelet.
- The natural extension of translations to the sphere are rotations. Rotation of a function f on the sphere is defined by

$$[\mathcal{R}(\rho)f](\omega) = f(\rho^{-1}\omega), \quad \omega = (\theta, \varphi) \in \mathrm{S}^2, \quad \rho = (\alpha, \beta, \gamma) \in \mathrm{SO}(3) \, .$$

- How define dilation on the sphere?
- The spherical dilation operator is defined through the conjugation of the Euclidean dilation and stereographic projection Π:

$$\mathcal{D}(a) \equiv \Pi^{-1} \, d(a) \, \Pi \, .$$

Continuous wavelets on the sphere

- First natural wavelet construction on the sphere was derived in the seminal work of Antoine and Vandergheynst (1998) (reintroduced by Wiaux 2005).
- Construct wavelet atoms from affine transformations (dilation, translation) on the sphere of a mother wavelet.
- The natural extension of translations to the sphere are rotations. Rotation of a function f on the sphere is defined by

$$[\mathcal{R}(\rho)f](\omega) = f(\rho^{-1}\omega), \quad \omega = (\theta, \varphi) \in S^2, \quad \rho = (\alpha, \beta, \gamma) \in SO(3) .$$

- How define dilation on the sphere?
- The spherical dilation operator is defined through the conjugation of the Euclidean dilation and stereographic projection Π:

$$\mathcal{D}(a) \equiv \Pi^{-1}\, d(a)\, \Pi .$$

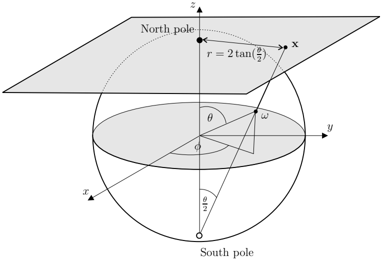

Figure: Stereographic projection.

Continuous wavelets on the sphere

- Wavelet frame on the sphere constructed from rotations and dilations of a mother spherical wavelet Φ:

$$\{\Phi_{a,\rho} \equiv \mathcal{R}(\rho)\mathcal{D}(a)\Phi \, : \, \rho \in \mathrm{SO}(3), \, a \in \mathbb{R}_*^+\}.$$

- The forward wavelet transform is given by

$$W_\Phi^f(a,\rho) = \langle f, \Phi_{a,\rho}\rangle = \int_{S^2} \mathrm{d}\Omega(\omega) \, f(\omega) \, \Phi_{a,\rho}^*(\omega) \, ,$$

where $\mathrm{d}\Omega(\omega) = \sin\theta \, \mathrm{d}\theta \, \mathrm{d}\varphi$ is the usual invariant measure on the sphere.

- Fast algorithms essential (for a review see Wiaux, JDM & Vielva 2007)
  - Factoring of rotations: JDM *et al.* (2007), Wandelt & Gorski (2001)
  - Separation of variables: Wiaux *et al.* (2005)

- The inverse wavelet transform given by

$$f(\omega) = \int_0^\infty \frac{\mathrm{d}a}{a^3} \int_{\mathrm{SO}(3)} \mathrm{d}\varrho(\rho) W_\Phi^f(a,\rho) \, [\mathcal{R}(\rho)\widehat{L}_\Phi \Phi_a](\omega) \, ,$$

provided wavelets satisfy an admissibility property.

- BUT...

Continuous wavelets on the sphere

- Wavelet frame on the sphere constructed from rotations and dilations of a mother spherical wavelet Φ:

$$\{\Phi_{a,\rho} \equiv \mathcal{R}(\rho)\mathcal{D}(a)\Phi \, : \, \rho \in \mathrm{SO}(3), \, a \in \mathbb{R}_*^+\}.$$

- The forward wavelet transform is given by

$$W_\Phi^f(a,\rho) = \langle f, \Phi_{a,\rho} \rangle = \int_{\mathrm{S}^2} \mathrm{d}\Omega(\omega) \, f(\omega) \, \Phi_{a,\rho}^*(\omega) \, ,$$

  where $\mathrm{d}\Omega(\omega) = \sin\theta \, \mathrm{d}\theta \, \mathrm{d}\varphi$ is the usual invariant measure on the sphere.

- Fast algorithms essential (for a review see Wiaux, JDM & Vielva 2007)
  - Factoring of rotations: JDM *et al.* (2007), Wandelt & Gorski (2001)
  - Separation of variables: Wiaux *et al.* (2005)

- The inverse wavelet transform given by

$$f(\omega) = \int_0^\infty \frac{\mathrm{d}a}{a^3} \int_{\mathrm{SO}(3)} \mathrm{d}\varrho(\rho) W_\Phi^f(a,\rho) \, [\mathcal{R}(\rho)\widehat{L}_\Phi \Phi_a](\omega) \, ,$$

  provided wavelets satisfy an admissibility property.

- BUT...

Continuous wavelets on the sphere

- Wavelet frame on the sphere constructed from rotations and dilations of a mother spherical wavelet Φ:

$$\{\Phi_{a,\rho} \equiv \mathcal{R}(\rho)\mathcal{D}(a)\Phi \, : \, \rho \in \mathrm{SO}(3), \, a \in \mathbb{R}_*^+\}.$$

- The forward wavelet transform is given by

$$W_\Phi^f(a,\rho) = \langle f, \Phi_{a,\rho} \rangle = \int_{S^2} \mathrm{d}\Omega(\omega) \, f(\omega) \, \Phi_{a,\rho}^*(\omega) \, ,$$

  where $\mathrm{d}\Omega(\omega) = \sin\theta \, \mathrm{d}\theta \, \mathrm{d}\varphi$ is the usual invariant measure on the sphere.

- Fast algorithms essential (for a review see Wiaux, JDM & Vielva 2007)
  - Factoring of rotations: JDM *et al.* (2007), Wandelt & Gorski (2001)
  - Separation of variables: Wiaux *et al.* (2005)

- The inverse wavelet transform given by

$$f(\omega) = \int_0^\infty \frac{\mathrm{d}a}{a^3} \int_{\mathrm{SO}(3)} \mathrm{d}\varrho(\rho) W_\Phi^f(a,\rho) \, [\mathcal{R}(\rho)\widehat{L}_\Phi \Phi_a](\omega) \, ,$$

  provided wavelets satisfy an admissibility property.

- BUT... **exact reconstruction not feasible in practice!**

Scale-discretised wavelets on the sphere

- Wiaux, JDM, Vandergheynst, Blanc (2008)
  Exact reconstruction with directional wavelets on the sphere
  S2DW code publicly available from: `http://www.jasonmcewen.org/`

- Dilation performed in harmonic space.
  Following JDM *et al.* (2006), Sanz *et al.* (2006).

- The scale-discretised wavelet $\Psi \in L^2(S^2, d\Omega)$ is defined in harmonic space:

$$\widehat{\Psi}_{\ell m} = \tilde{K}_{\Psi}(\ell) S^{\Psi}_{\ell m} \ .$$

- Construct wavelets to satisfy a resolution of the identity for $0 \leq \ell < L$:

$$\tilde{\Phi}^2_{\Psi}(\alpha^J \ell) + \sum_{j=0}^{J} \tilde{K}^2_{\Psi}(\alpha^j \ell) = 1 .$$

Scale-discretised wavelets on the sphere

- Wiaux, JDM, Vandergheynst, Blanc (2008)
  Exact reconstruction with directional wavelets on the sphere
  S2DW code publicly available from: `http://www.jasonmcewen.org/`

- Dilation performed in harmonic space.
  Following JDM *et al.* (2006), Sanz *et al.* (2006).
- The scale-discretised wavelet $\Psi \in L^2(S^2, d\Omega)$ is defined in harmonic space:

$$\widehat{\Psi}_{\ell m} = \tilde{K}_\Psi(\ell) S^\Psi_{\ell m} .$$

- Construct wavelets to satisfy a resolution of the identity for $0 \le \ell < L$:

$$\tilde{\Phi}^2_\Psi(\alpha^J \ell) + \sum_{j=0}^{J} \tilde{K}^2_\Psi(\alpha^j \ell) = 1 .$$

Scale-discretised wavelets on the sphere

- Wiaux, JDM, Vandergheynst, Blanc (2008)
  Exact reconstruction with directional wavelets on the sphere
  S2DW code publicly available from: `http://www.jasonmcewen.org/`

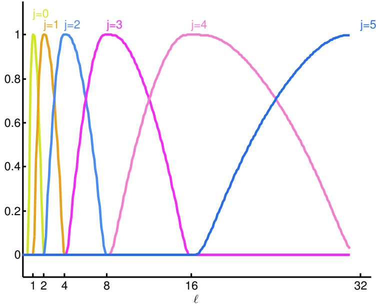

Figure: Harmonic tiling on the sphere.

- Dilation performed in harmonic space.
  Following JDM *et al.* (2006), Sanz *et al.* (2006).
- The scale-discretised wavelet $\Psi \in \mathrm{L}^2(\mathrm{S}^2, \mathrm{d}\Omega)$ is defined in harmonic space:

$$\widehat{\Psi}_{\ell m} = \tilde{K}_\Psi(\ell) S^\Psi_{\ell m} \ .$$

- Construct wavelets to satisfy a resolution of the identity for $0 \leq \ell < L$:

$$\tilde{\Phi}^2_\Psi(\alpha^J \ell) + \sum_{j=0}^{J} \tilde{K}^2_\Psi(\alpha^j \ell) = 1 .$$

Scale-discretised wavelets

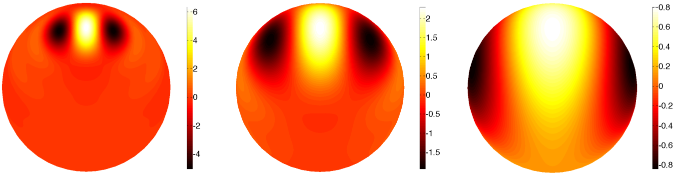

Figure: Spherical scale-discretised wavelets.

- The scale-discretised wavelet transform is given by the usual projection onto each wavelet:

$$W^f_\Psi(\rho, \alpha^j) = \langle f, \Psi_{\rho,\alpha^j} \rangle = \int_{S^2} d\Omega(\omega) \, f(\omega) \, \Psi^*_{\rho,\alpha^j}(\omega) \, .$$

- The original function may be recovered exactly in practice from the wavelet (and scaling) coefficients:

$$f(\omega) = [\Phi_{\alpha^J} f](\omega) + \sum_{j=0}^{J} \int_{SO(3)} d\varrho(\rho) \, W^f_\Psi\left(\rho, \alpha^j\right) \left[R(\rho) \, L^d \Psi_{\alpha^j}\right](\omega) \, .$$

Scale-discretised wavelets

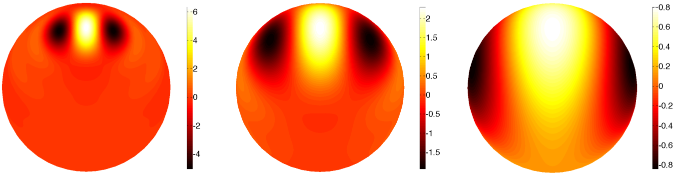

Figure: Spherical scale-discretised wavelets.

- The scale-discretised wavelet transform is given by the usual projection onto each wavelet:

$$W^f_\Psi(\rho, \alpha^j) = \langle f, \Psi_{\rho,\alpha^j} \rangle = \int_{S^2} \mathrm{d}\Omega(\omega)\, f(\omega)\, \Psi^*_{\rho,\alpha^j}(\omega) \ .$$

- The original function may be recovered exactly in practice from the wavelet (and scaling) coefficients:

$$f(\omega) = [\Phi_{\alpha^J} f](\omega) + \sum_{j=0}^{J} \int_{SO(3)} \mathrm{d}\varrho(\rho)\, W^f_\Psi(\rho, \alpha^j) \left[R(\rho) L^\mathrm{d} \Psi_{\alpha^j} \right](\omega) \ .$$

Scale-discretised wavelets

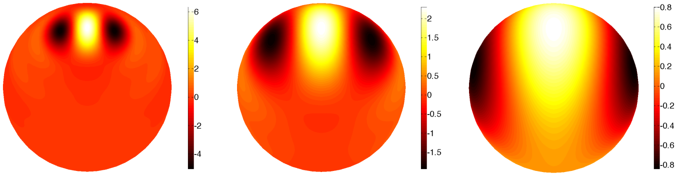

Figure: Spherical scale-discretised wavelets.

- The scale-discretised wavelet transform is given by the usual projection onto each wavelet:

$$W^f_\Psi(\rho, \alpha^j) = \langle f, \Psi_{\rho,\alpha^j} \rangle = \int_{S^2} \mathrm{d}\Omega(\omega)\, f(\omega)\, \Psi^*_{\rho,\alpha^j}(\omega) .$$

- The original function may be recovered exactly in practice from the wavelet (and scaling) coefficients:

$$f(\omega) = \left[\Phi_{\alpha^J} f\right](\omega) + \sum_{j=0}^{J} \int_{\mathrm{SO}(3)} \mathrm{d}\varrho(\rho)\, W^f_\Psi\left(\rho, \alpha^j\right) \left[R(\rho)\, L^{\mathrm{d}} \Psi_{\alpha^j}\right](\omega) .$$

Outline

Motivation for using wavelets to detect cosmic strings

- Adopt the scale-discretised wavelet transform on the sphere (Wiaux, JDM *et al.* 2008), where we denote the wavelet coefficients of the data d by $\boxed{W^d_{j\rho} = \langle d, \Psi_{j\rho} \rangle}$ for scale $j \in \mathbb{Z}^+$ and position $\rho \in \mathrm{SO}(3)$.
- Consider an even azimuthal band-limit $N = 4$ to yield wavelet with odd azimuthal symmetry.

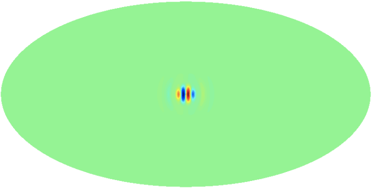

Figure: Example wavelet.

- Wavelet transform yields a sparse representation of the string signal $\rightarrow$ hope to effectively separate the CMB and string signal in wavelet space.

Motivation for using wavelets to detect cosmic strings

- Adopt the scale-discretised wavelet transform on the sphere (Wiaux, JDM *et al.* 2008), where we denote the wavelet coefficients of the data d by $\boxed{W^d_{j\rho} = \langle d,\ \Psi_{j\rho} \rangle}$ for scale $j \in \mathbb{Z}^+$ and position $\rho \in \mathrm{SO}(3)$.
- Consider an even azimuthal band-limit $N = 4$ to yield wavelet with odd azimuthal symmetry.

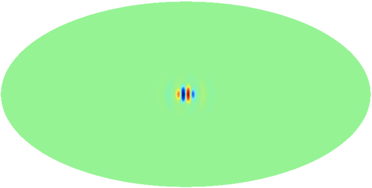

Figure: Example wavelet.

- Wavelet transform yields a sparse representation of the string signal $\rightarrow$ hope to effectively separate the CMB and string signal in wavelet space.

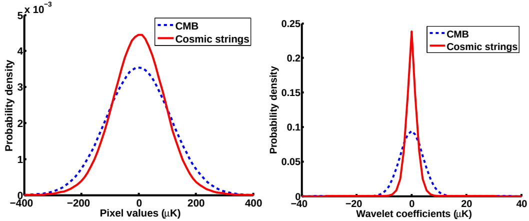

Figure: Distribution of CMB and string signal in pixel (left) and wavelet space (right).

Learning the statistics of the CMB and string signals in wavelet space

- Need to determine statistical description of the CMB and string signals in wavelet space.
- Calculate analytically the probability distribution of the CMB in wavelet space:

$$\mathrm{P}_j^c(W_{j\rho}^c) = \frac{1}{\sqrt{2\pi(\sigma_j^c)^2}} \exp\left(-\frac{1}{2}\left(\frac{W_{j\rho}^c}{\sigma_j^c}\right)^2\right), \quad \text{where} \quad (\sigma_j^c)^2 = \langle W_{j\rho}^c W_{j\rho}^{c\,*} \rangle = \sum_{\ell m} C_\ell |(\Psi_j)_{\ell m}|^2 .$$

- Fit a generalised Gaussian distribution (GGD) for the wavelet coefficients of a string training map (*cf.* Wiaux *et al.* 2009):

$$\mathrm{P}_j^s(W_{j\rho}^s \mid G\mu) = \frac{\upsilon_j}{2G\mu\nu_j\Gamma(\upsilon_j^{-1})} \exp\left(-\left|\frac{W_{j\rho}^s}{G\mu\nu_j}\right|^{\upsilon_j}\right),$$

with scale parameter ν_j and shape parameter υ_j.

Learning the statistics of the CMB and string signals in wavelet space

- Need to determine statistical description of the CMB and string signals in wavelet space.
- Calculate analytically the probability distribution of the CMB in wavelet space:

$$\mathrm{P}_j^c(W_{j\rho}^c) = \frac{1}{\sqrt{2\pi(\sigma_j^c)^2}} \exp\left(-\frac{1}{2}\left(\frac{W_{j\rho}^c}{\sigma_j^c}\right)^2\right), \quad \text{where} \quad (\sigma_j^c)^2 = \langle W_{j\rho}^c W_{j\rho}^{c\,*} \rangle = \sum_{\ell m} C_\ell |(\Psi_j)_{\ell m}|^2 .$$

- Fit a generalised Gaussian distribution (GGD) for the wavelet coefficients of a string training map (*cf.* Wiaux *et al.* 2009):

$$\mathrm{P}_j^s(W_{j\rho}^s \mid G\mu) = \frac{\upsilon_j}{2G\mu\nu_j\Gamma(\upsilon_j^{-1})} \exp\left(-\left|\frac{W_{j\rho}^s}{G\mu\nu_j}\right|^{\upsilon_j}\right),$$

with scale parameter ν_j and shape parameter υ_j.

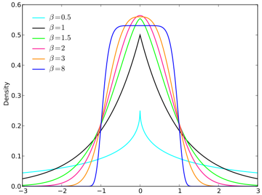

Figure: Generalised Gaussian distribution (GGD).

Learning the statistics of the CMB and string signals in wavelet space

- Require two simulated string maps: one for training; one for testing.

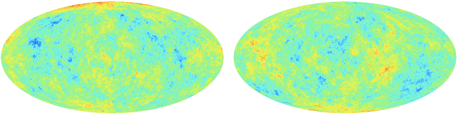

(a) String1 (b) String2

Figure: Cosmic string simulations.

- Compare distribution learnt from the training simulation (string2) with the distribution of the testing simulation (string1).
- Distributions in close agreement.

Learning the statistics of the CMB and string signals in wavelet space

- Require two simulated string maps: one for training; one for testing.

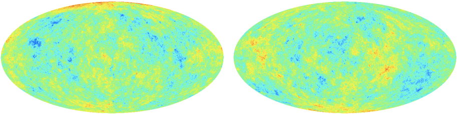

(a) String1 (b) String2

Figure: Cosmic string simulations.

- Compare distribution learnt from the training simulation (string2) with the distribution of the testing simulation (string1).
- Distributions in close agreement.

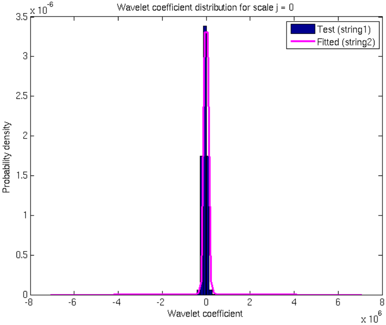

Figure: Distributions for wavelet scale $j = 0$.

Learning the statistics of the CMB and string signals in wavelet space

- Require two simulated string maps: one for training; one for testing.

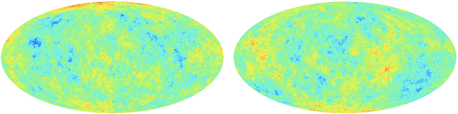

(a) String1 (b) String2

Figure: Cosmic string simulations.

- Compare distribution learnt from the training simulation (string2) with the distribution of the testing simulation (string1).
- Distributions in close agreement.

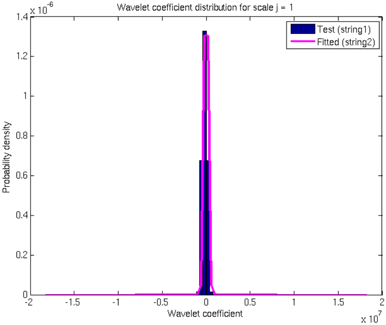

Figure: Distributions for wavelet scale $j = 1$.

Learning the statistics of the CMB and string signals in wavelet space

- Require two simulated string maps: one for training; one for testing.

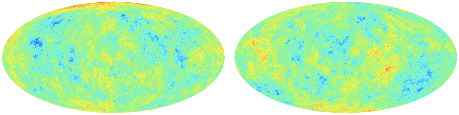

(a) String1 (b) String2

Figure: Cosmic string simulations.

- Compare distribution learnt from the training simulation (string2) with the distribution of the testing simulation (string1).
- Distributions in close agreement.

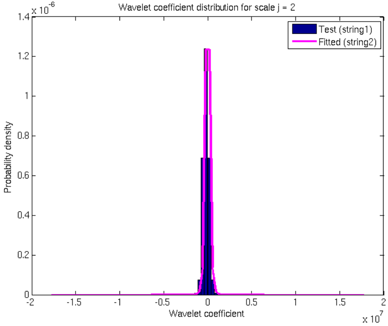

Figure: Distributions for wavelet scale $j = 2$.

Learning the statistics of the CMB and string signals in wavelet space

- Require two simulated string maps: one for training; one for testing.

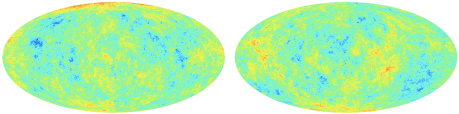

(a) String1 (b) String2

Figure: Cosmic string simulations.

- Compare distribution learnt from the training simulation (string2) with the distribution of the testing simulation (string1).
- Distributions in close agreement.

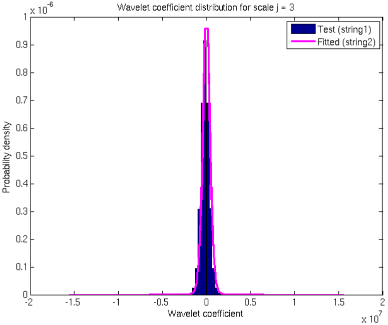

Figure: Distributions for wavelet scale $j = 3$.

Learning the statistics of the CMB and string signals in wavelet space

- Require two simulated string maps: one for training; one for testing.

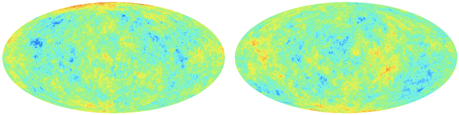

(a) String1 (b) String2

Figure: Cosmic string simulations.

- Compare distribution learnt from the training simulation (string2) with the distribution of the testing simulation (string1).
- Distributions in close agreement.

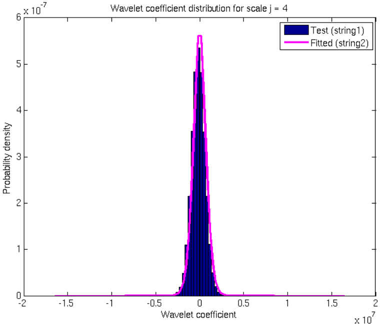

Figure: Distributions for wavelet scale $j = 4$.

Learning the statistics of the CMB and string signals in wavelet space

- Require two simulated string maps: one for training; one for testing.

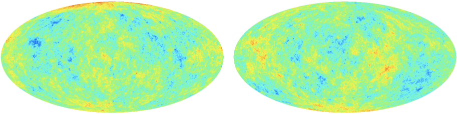

(a) String1 (b) String2

Figure: Cosmic string simulations.

- Compare distribution learnt from the training simulation (string2) with the distribution of the testing simulation (string1).
- Distributions in close agreement.
- We have accurately characterised the statistics of string signals in wavelet space.

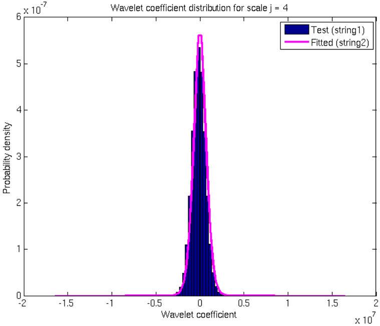

Figure: Distributions for wavelet scale $j = 4$.

Spherical wavelet-Bayesian string tension estimation

- We take a Bayesian approach to string tension estimation.
- Perform Bayesian string tension estimation in wavelet space, where the CMB and string distributions are very different.
- For each wavelet coefficient the likelihood is given by

$$P(W^d_{j\rho} \mid G\mu) = P(W^s_{j\rho} + W^c_{j\rho} \mid G\mu) = \int_{\mathbb{R}} \mathrm{d}W^s_{j\rho} \, P^c_j(W^d_{j\rho} - W^s_{j\rho}) \, P^s_j(W^s_{j\rho} \mid G\mu) \, .$$

- The overall likelihood of the data is given by

$$P(W^d \mid G\mu) = \prod_{j,\rho} P(W^d_{j\rho} \mid G\mu) \, ,$$

  where we have assumed each wavelet coefficient is independent.
- The wavelet coefficients are not independent but to incorporate the covariance of wavelet coefficients would be computationally infeasible.
- Instead, we compute the correlation length of wavelet coefficients, and only fold into the likelihood calculation wavelet coefficients that are at least a correlation length apart.
- Empirically we have found this approach to work well.

Spherical wavelet-Bayesian string tension estimation

- We take a Bayesian approach to string tension estimation.
- Perform Bayesian string tension estimation in wavelet space, where the CMB and string distributions are very different.
- For each wavelet coefficient the likelihood is given by

$$\mathrm{P}(W^d_{j\rho} \,|\, G\mu) = \mathrm{P}(W^s_{j\rho} + W^c_{j\rho} \,|\, G\mu) = \int_{\mathbb{R}} \mathrm{d}W^s_{j\rho} \; \mathrm{P}^c_j(W^d_{j\rho} - W^s_{j\rho}) \; \mathrm{P}^s_j(W^s_{j\rho} \,|\, G\mu) \; .$$

- The overall likelihood of the data is given by

$$\mathrm{P}(W^d \,|\, G\mu) = \prod_{j,\rho} \mathrm{P}(W^d_{j\rho} \,|\, G\mu) \; ,$$

where we have assumed each wavelet coefficient is independent.

- The wavelet coefficients are not independent but to incorporate the covariance of wavelet coefficients would be computationally infeasible.
- Instead, we compute the correlation length of wavelet coefficients, and only fold into the likelihood calculation wavelet coefficients that are at least a correlation length apart.
- Empirically we have found this approach to work well.

Spherical wavelet-Bayesian string tension estimation

- We take a Bayesian approach to string tension estimation.
- Perform Bayesian string tension estimation in wavelet space, where the CMB and string distributions are very different.
- For each wavelet coefficient the likelihood is given by

$$\mathrm{P}(W^d_{j\rho} \mid G\mu) = \mathrm{P}(W^s_{j\rho} + W^c_{j\rho} \mid G\mu) = \int_{\mathbb{R}} \mathrm{d}W^s_{j\rho} \, \mathrm{P}^c_j(W^d_{j\rho} - W^s_{j\rho}) \, \mathrm{P}^s_j(W^s_{j\rho} \mid G\mu) \, .$$

- The overall likelihood of the data is given by

$$\mathrm{P}(W^d \mid G\mu) = \prod_{j,\rho} \mathrm{P}(W^d_{j\rho} \mid G\mu) \, ,$$

  where we have assumed each wavelet coefficient is independent.
- The wavelet coefficients are not independent but to incorporate the covariance of wavelet coefficients would be computationally infeasible.
- Instead, we compute the correlation length of wavelet coefficients, and only fold into the likelihood calculation wavelet coefficients that are at least a correlation length apart.
- Empirically we have found this approach to work well.

Spherical wavelet-Bayesian string tension estimation

- We compute the string tension posterior $\mathrm{P}(G\mu \mid W^d)$ by Bayes theorem:

$$\mathrm{P}(G\mu \mid W^d) = \frac{\mathrm{P}(W^d \mid G\mu)\,\mathrm{P}(G\mu)}{\mathrm{P}(W^d)} \propto \mathrm{P}(W^d \mid G\mu)\,\mathrm{P}(G\mu)\;.$$

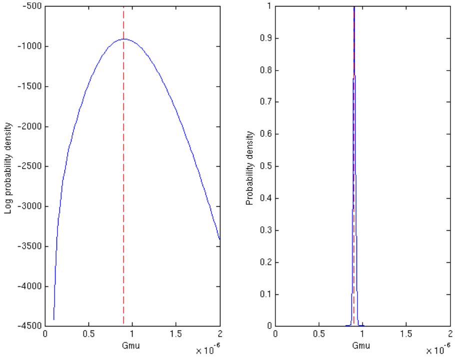

Figure: Posterior distribution of the string tension (true $G\mu = 9 \times 10^{-7}$).

Spherical wavelet-Bayesian string tension estimation

- We compute the string tension posterior $\mathrm{P}(G\mu \mid W^d)$ by Bayes theorem:

$$\mathrm{P}(G\mu \mid W^d) = \frac{\mathrm{P}(W^d \mid G\mu)\, \mathrm{P}(G\mu)}{\mathrm{P}(W^d)} \propto \mathrm{P}(W^d \mid G\mu)\, \mathrm{P}(G\mu) \ .$$

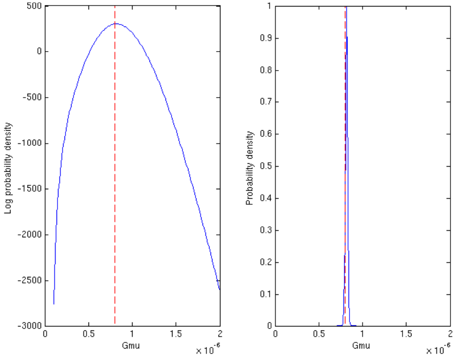

Figure: Posterior distribution of the string tension (true $G\mu = 8 \times 10^{-7}$).

Spherical wavelet-Bayesian string tension estimation

- We compute the string tension posterior $\mathrm{P}(G\mu \mid W^d)$ by Bayes theorem:

$$\mathrm{P}(G\mu \mid W^d) = \frac{\mathrm{P}(W^d \mid G\mu)\,\mathrm{P}(G\mu)}{\mathrm{P}(W^d)} \propto \mathrm{P}(W^d \mid G\mu)\,\mathrm{P}(G\mu)\ .$$

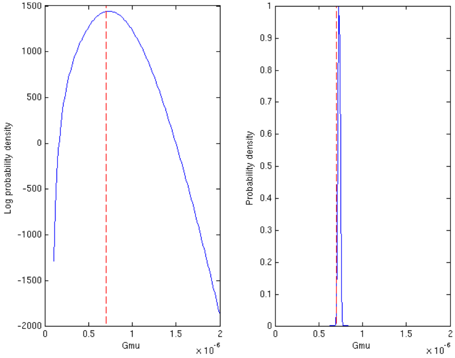

Figure: Posterior distribution of the string tension (true $G\mu = 7 \times 10^{-7}$).

Spherical wavelet-Bayesian string tension estimation

- We compute the string tension posterior $\mathrm{P}(G\mu \mid W^d)$ by Bayes theorem:

$$\mathrm{P}(G\mu \mid W^d) = \frac{\mathrm{P}(W^d \mid G\mu)\,\mathrm{P}(G\mu)}{\mathrm{P}(W^d)} \propto \mathrm{P}(W^d \mid G\mu)\,\mathrm{P}(G\mu)\ .$$

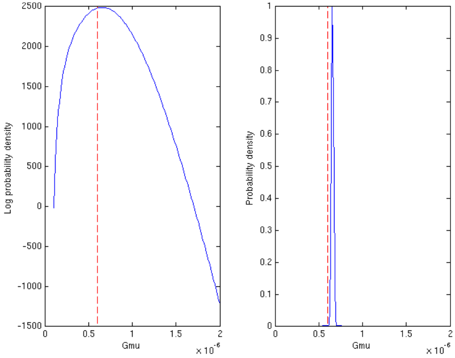

Figure: Posterior distribution of the string tension (true $G\mu = 6 \times 10^{-7}$).

Spherical wavelet-Bayesian string tension estimation

- We compute the string tension posterior $\mathrm{P}(G\mu \mid W^d)$ by Bayes theorem:

$$\mathrm{P}(G\mu \mid W^d) = \frac{\mathrm{P}(W^d \mid G\mu)\,\mathrm{P}(G\mu)}{\mathrm{P}(W^d)} \propto \mathrm{P}(W^d \mid G\mu)\,\mathrm{P}(G\mu)\ .$$

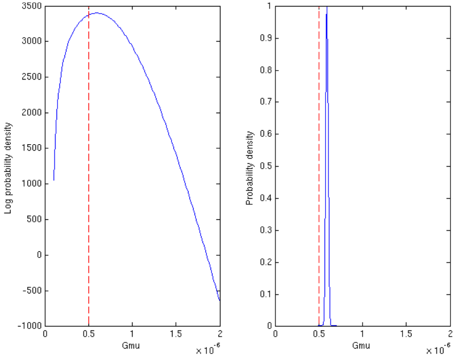

Figure: Posterior distribution of the string tension (true $G\mu = 5 \times 10^{-7}$).

Spherical wavelet-Bayesian string tension estimation

- We compute the string tension posterior $\mathrm{P}(G\mu \mid W^d)$ by Bayes theorem:

$$\mathrm{P}(G\mu \mid W^d) = \frac{\mathrm{P}(W^d \mid G\mu)\,\mathrm{P}(G\mu)}{\mathrm{P}(W^d)} \propto \mathrm{P}(W^d \mid G\mu)\,\mathrm{P}(G\mu)\ .$$

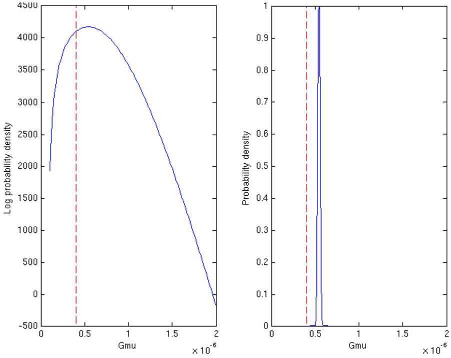

Figure: Posterior distribution of the string tension (true $G\mu = 4 \times 10^{-7}$).

Bayesian evidence for strings

- Compute Bayesian evidences to compare the string model M^s discussed so far to the alternative model M^c that the observed data is comprised of just a CMB contribution.
- The Bayesian evidence of the string model is given by

$$E^s = \mathrm{P}(W^d \mid \mathrm{M}^s) = \int_{\mathbb{R}} \mathrm{d}(G\mu)\, \mathrm{P}(W^d \mid G\mu)\, \mathrm{P}(G\mu) \; .$$

- The Bayesian evidence of the CMB model is given by

$$E^c = \mathrm{P}(W^d \mid \mathrm{M}^c) = \prod_{j,\rho} \mathrm{P}^c_j(W^d_{j\rho}) \; .$$

- Compute the Bayes factor to determine the preferred model:

$$\Delta \ln E = \ln(E^s / E^c) = \ln E^s - \ln E^c \; .$$

Bayesian evidence for strings

- Compute Bayesian evidences to compare the string model M^s discussed so far to the alternative model M^c that the observed data is comprised of just a CMB contribution.
- The Bayesian evidence of the string model is given by

$$E^s = \mathrm{P}(W^d \mid \mathrm{M}^s) = \int_{\mathbb{R}} \mathrm{d}(G\mu)\, \mathrm{P}(W^d \mid G\mu)\, \mathrm{P}(G\mu) \; .$$

- The Bayesian evidence of the CMB model is given by

$$E^c = \mathrm{P}(W^d \mid \mathrm{M}^c) = \prod_{j,\rho} \mathrm{P}_j^c(W_{j\rho}^d) \; .$$

- Compute the Bayes factor to determine the preferred model:

$$\Delta \ln E = \ln(E^s / E^c) = \ln E^s - \ln E^c \; .$$

Table: Log-evidence differences for a particular simulation.

$G\mu/10^{-7}$	2	3	4	5	6	7	8	9
$\Delta \ln E$	-278	-233	-164	-56	104	341	677	1132

Summary

- Developed a hybrid wavelet-Bayesian method to test for the existence of cosmic strings.
- Perform analysis in wavelet space where the string and CMB signals have very different statistical distributions.

- ToDo: Recover denoised string maps (*cf.* Wiaux *et al.* 2009).
- ToDo: Assess the sensitivity of our approach on more realistic simulations.
- ToDo: **Apply to Planck observations to test for the existence of cosmic strings!**

Summary

- Developed a hybrid wavelet-Bayesian method to test for the existence of cosmic strings.
- Perform analysis in wavelet space where the string and CMB signals have very different statistical distributions.

- ToDo: Recover denoised string maps (*cf.* Wiaux *et al.* 2009).
- ToDo: Assess the sensitivity of our approach on more realistic simulations.
- ToDo: **Apply to Planck observations to test for the existence of cosmic strings!**